TEKSTİL VE KONFEKSİYON
VOL: 30, NO. 4
DOI: 10.32710/tekstilvekonfeksiyon.699529

Sound-Absorption Properties of Composite Materials Containing Waste-Wool / Polyamide Fibers and Their Relationship with Fractal Dimensions

Lihua Lyu*, Jing Lu, Yongfang Qian, Hong Li, Changwei Li, Jing Guo

School of Textile and Material Engineering, Dalian Polytechnic University, Dalian 116034, P.R. China

Corresponding Author: Corresponding Author: Lihua Lyu, lvlh@dlpu.edu.cn

ABSTRACT

To solve the problems related to the recycling of waste fibers, composite materials were prepared by the hot-pressing method using waste-wool fibers and waste low-melting-point polyamide fibers combined into a net as the raw materials. The effects of the volume density, mass fraction of waste-wool fibers, and thickness on the sound-absorption properties of the resulting composite materials were studied by the controlling-variable method. The sound-absorption properties of the composite materials were studied by the transfer-function method, and under optimized technological conditions, the sound-absorption coefficients were above 0.8 and the sound-absorption bands were wide. According to the box-counting-dimension method, which is based on the fractal theory, the fractal dimensions of the composite materials were calculated using the Matlab program. The relationships between the fractal dimensions and the volume densities, mass fractions of waste-wool fibers, and thicknesses of the composite materials were also analyzed. Then, quantitative relationships between the fractal dimension and the maximum sound-absorption coefficient, and between the fractal dimension and the resonant sound-absorption frequency, which play a major role in the sound-absorption design of composite materials, were deduced.

ARTICLE HISTORY
Received: 06.03.2020
Accepted: 24.11.2020

KEYWORDS

Waste-wool fibers, waste polyamide fibers, composite material, sound absorption properties, fractal dimension

1. INTRODUCTION

China is currently the world's largest wool producer and sheep breeder, and it is also one of the countries with the largest wool consumption and import volume [1]. According to statistics, China's annual wool production is stable at about 400,000 tons, while the annual waste accounts for 40% of the world's annual waste [2]. However, these waste-wool resources have not yet been rationally utilized, which not only causes a terrible waste but also requires landfill disposal, causing serious environmental pollution, threatening human health, and posing a hidden risk of fire. Therefore, finding a way to recycle the waste-wool fibers has become an attractive research topic.

As early as the 1990s, Japanese scholars studied the use of waste-wool fibers. Then they made composite materials based on waste-wool and feathers by hot pressing and tested the bending strength of the materials to open up a new direction for the reuse of waste-wool fibers [3]. Alzeer et al. [4] used an aluminosilicate inorganic polymer and wool fibers to prepare a new fiber-reinforced composite material and measured its mechanical properties. Patnaik et al. [5] used wool fibers and regenerated polyester fibers (RPET) as raw materials to prepare nonwoven products. To meet the requirements of materials in the construction industry in terms of fire and moisture resistance, a flame-retardant and moisture-resistant finishing was carried out on the fibers, and the recyclability and biodegradability of the samples were ensured, which provided a new idea for the

To cite this article: *Lyu L, Lu J, Qian Y, Li H, Li C, Guo J. 2020. Sound-absorption properties of composite materials containing waste-wool / polyamide fibers and their relationship with fractal dimensions. Tekstil ve Konfeksiyon, 30(4), 276-288.*

reuse of waste-wool fibers in the future. Li et al. [6] prepared an ultra-short waste-wool-fiber nonwoven fabric by a wet nonwoven process. To improve the recovery rate of waste-wool fibers, He et al. [7] developed a quality-control method and a technology suitable for mass production. This method was mainly a physical method and did not damage the wool microstructure. At present, the conventional treatment is based on chemical methods, such as that by Yao et al. [8-10] who devoted themselves to the study of wool keratin, continuously optimizing and perfecting the process of wool-keratin solution, and summarizing the progress of wool-keratin dissolution and recycling. Li et al. [11] used a self-made ionic liquid to dissolve wool and cellulose to produce a blend film with excellent flame-retardant properties and compatibility. The keratin-based industrial production of waste-wool fibers by hydrolysis is very difficult and costly. In addition, LV et al. [12, 13] prepared flame retardant waste fiber/polyurethane insulation and flame retardant waste corn husk fiber/polylactic acid composites by blending-hot pressing method. At present, the development of waste-wool fibers is mostly concentrated in the above fields. With the aggravation of noise pollution, the fabrication of sound-absorbing materials containing waste fibers is also beginning to rise. From the acoustic point of view, wool fiber has a smaller density, compared to other natural fibers, has a certain curliness, and is easy to be clustered together to form a large number of interconnected pores, which provides favorable conditions for the preparation of porous sound-absorbing materials. Zhejiang University scholars studied the acoustic and thermal properties of this series of wool products. Recently, Cheng et al. [14] studied a kind of thermally insulating and sound-absorbing material that combines a net formed by mixing natural fibers with hot-melt fibers and a flame-retardant adhesive layer. There are some articles [15-17] on wool-based sound-absorbing materials, and the noise-reduction coefficients of the prepared wool-based sound-absorbing materials were all above 0.6, but the sound-absorbing mechanism of wool has not been thoroughly studied.

The word “fractal” is derived from the Latin “fractious” and means fragmented. A fractal is defined as a mathematical object with a fractional (non-integer) dimension. It seems that wherever there is structural disorder and chaos, fractal geometry can be an efficient way of describing and analyzing the system. The fractal dimension is a very good mathematical method for studying unequal geometric substances and can reflect characteristics appearing in nature. The application of a fractal system allows us to explain numerous states of fragmenting and branching occurring in ecological, biological, and other systems [18-21]. The inside of a nonwoven fabric [22], a fiber-reinforced composite material [23, 24], a fiber aggregate [25], or a similar substance is characterized by a porous body composed of fibers and pores. The pore shapes are not regular or smooth, the pore sizes are also different, and there is no characteristic dimension that can indicate the internal pore structure [22]. Fractal geometry is a new tool to simulate irregular pore structures of materials. The relationship between the fractal dimension and the structural parameters of porous materials can be obtained through fractal image processing and mathematical calculations. The larger the fractal dimension, the rougher the pore surface or the more complex the pore structure [26]. Fractal theory is applied to quantitatively analyze the structure and characteristics of materials, making the structural analysis of materials more intuitive.

Herein, a composite material was prepared using waste-wool fibers and waste low-melting-point polyamide fibers as raw materials by combing them into a net and applying the hot-pressing method. The effects of the volume density of the composite material, the mass fraction of the waste-wool fibers, and the thickness of the composite material on the sound-absorption coefficient curve were carefully analyzed by single-factor experiments. The sound absorption curves of composites were given. But, at low thickness values, the composites show very low sound absorption behavior especially at low and medium frequency ranges. Noise in application areas such automotive, panels lies in the in the acoustic range between 100 and 2000 Hz. The sound absorption characteristics obtained over the frequency of 2000 Hz are not significant for these end-uses. According to the self-similarity, the quantitative relationships between fractal dimension and maximum sound-absorption coefficient, and between fractal dimension and resonant sound-absorption frequency were deduced by the box-counting method.

2. MATERIALS AND METHODS

2.1 Materials and Equipment

The type of waste wool was sweeping wool. Waste-wool fibers with an average length of 30–70 mm, diameter of 15-30μm and a density of 1.384 $g \cdot cm^{-3}$ (Fudi Wool Textile Factory, Shandong, China) and waste low-melting-point polyamide fibers with a density of 1.14 $g \cdot cm^{-3}$, an average length of 60–70 mm, and a melting point 100°C (Kaitai Special Fiber Technology Co., Ltd., Zhejiang, China) were used as the raw materials. A DSCa-01 digital sample carding machine (provided by Jiacheng Mechanical and Electrical Equipment Co., Ltd., Tianjin), an MP2000D Shanghai Jingke Analytical Balance (Tianma Instrument Factory, Tianjin), a QLB-50D/Q hot-pressing machine (provided by Zhongkai Rubber Machinery Co., Ltd., Jiangsu), an SW422/SW477 impedance-tube sound-absorption test system (provided by Shengwang company, Beijing), and a JEOL JSM-6460LV scanning electron microscope (provided by JEOL Ltd. Japan) were used for testing.

2.2 Preparation of the Composite Materials

The composite materials were prepared by combing the raw materials, that is, the waste-wool fibers and the waste low-

melting-point polyamide fibers, into a net and applying the hot-pressing method. The waste-wool fibers and waste low-melting-point polyamide fibers were mixed in a certain proportion using a digital sample carding machine and heated to 110°C at 10 MPa for 30 min using a QLB-50D/Q hot-pressing machine. Cmposite materials with mass fractions of waste-wool fibers of 0%, 30%, 40%, 50%, 60%, 70%, and 100% were prepared. Then, the composite materials were formed and test samples were prepared as disc-shaped composites with sizes of Φ100 × 5 mm, Φ100 × 10 mm, Φ100 × 15 mm, Φ100 × 20 mm, Φ100 × 25 mm, Φ100 × 30 mm, and Φ100 × 35 mm.

2.3 Testing of the Composite Materials

2.3.1 Testing of the Sound-Absorption Coefficient

Testing of the sound-absorption coefficient was done according to the standard GB/T 18696.2-2 002 and GB/T 186 96.1-2004. Under the conditions of atmospheric temperature (24°C), velocity of sound wave (345.6 m/s), a characteristic impedance of air of 409.78 Pa·s/m, and a relative humidity of 65%, the sound-absorption coefficient curves of the samples were tested using an SW422/SW477 impedance-tube sound-absorption test system [27]. The measured sound-absorption coefficient curve was the average of six measurements. Figure 1 shows a schematic diagram of the sound-absorption test.

2.3.2 Calculation of the Porosity

The sound-absorption performance of the composite material was closely related to the porosity, which can be indirectly calculated according to the thickness and areal density of the sample [28]. The porosity of the sample was calculated using equation 1:

$$\eta\% = \left(1 - \frac{G}{\rho \times \sigma}\right) \times 100 \qquad (1)$$

where η is the porosity of the sample (%), G is the surface density of the sample (g·cm^{-2}), ρ is the mixed specific gravity of the fibers (g·cm^{-3}), and σ is the thickness of the sample (m).

2.3.3 Fractal Characterization

The surface morphology of the samples was studied using a JEOL JSM-6460LV scanning electron microscope, and the pixel size of the intercepted images was 1024 × 1024. The software Photoshop was used to process the gray levels of the obtained scanning electron microscope images, and an image threshold was set. Then, the image with gray levels was converted into a binary image that could be recognized by the computer, and the box-counting method [29] was applied to calculate the fractal dimension of the sample using the Matlab program (the procedure is described in annex A).

The calculation principle of the box-counting dimension method is based on taking a small cube box with an edge length of ε and covering the curve graph with fractal characteristics. Some boxes are empty, some boxes contain a part of the curve, and the number of boxes containing the curve is recorded as N (ε). Then, the size of the box is shortened and N (ε) increases correspondingly. If ε is close to 0, the fractal dimension of the curve can be obtained using equation 2:

$$D = -\lim_{\varepsilon \to 0} \frac{\log N(\varepsilon)}{\log \varepsilon} \qquad (2)$$

However, in the actual calculation process, the value of ε is not infinite; it is finite. By fitting and mapping with the least-square method, a straight line is obtained, and the fractal dimension is given by the slope of that straight line. For the box-counting dimension analysis of two-dimensional digital images, Matlab offers a rich visual graphic representation function and a convenient programming ability [30], so Matlab was used for image processing, numerical analysis, and other operations.

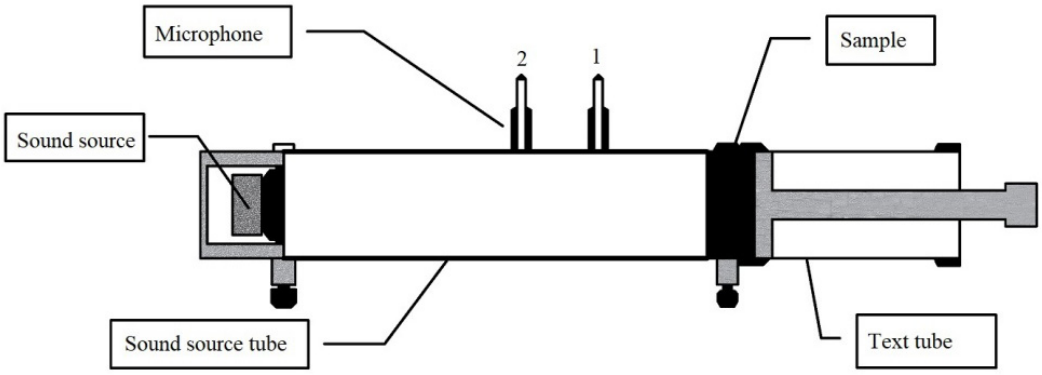

Figure 1. Schematic diagram of the sound-absorption test

3. RESULTS AND DISCUSSION

3.1 Effect of the Technological Parameters on the Sound-Absorption Coefficient

3.1.1 Effect of the Volume Density on the Sound-Absorption Coefficient

Under technological conditions consisting of a mass fraction of waste-wool fibers of 50% and a material thickness of 10 mm, composite materials with densities of 0.153, 0.191, 0.229, 0.267, and 0.306 g·cm^{-3} were prepared. Figure 2 shows the calculated porosity of the composite materials for different volume densities. Figure 2 shows that with an increase in the volume density of the composite materials, the porosity decreased from 88.06% to 76.13%. The reason might be that as the volume density increases, the number of fibers per unit volume increases, and the porosity between the fibers decreases; thus, the porosity of the composite materials decreases too.

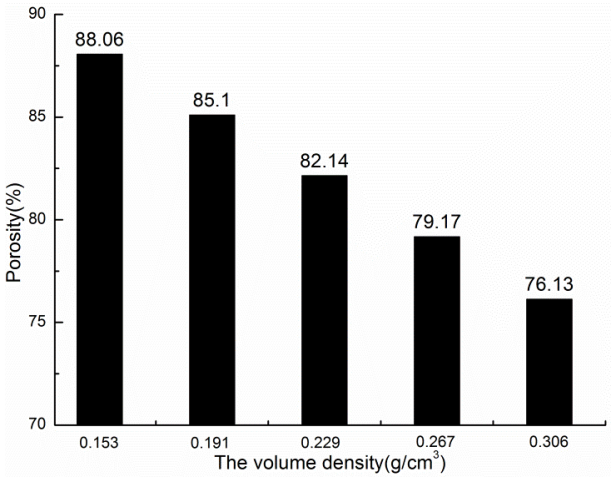

Figure 2. Porosity of composite materials with different volume densities

Figure 3 shows the measured sound-absorption coefficient curves of composite materials with different densities. It can be seen from Figure 3 that as the density increases, the peak of the sound-absorption coefficient gradually moves in the low-frequency direction. When the volume density was 0.229 g·cm^{-3}, the peak appeared in the test range, and the maximum sound-absorption coefficient was obtained [31]. To sum up, when the volume density of the composite materials was 0.229 g·cm^{-3}, the sound-absorption performance at high frequencies was the best, the maximum sound-absorption coefficient could reach 0.96, and the sound-absorption frequency band was wide, so the volume density of the composite materials was 0.229 g·cm^{-3}.

This is because as the density increased, the porosity of the material decreased, which reduced the pore size and the number of micro-pores in the material, increasing both the friction and the vibration between air and the fibers in the material, thus increasing the consumption of acoustic energy and the sound-absorption performance. However, if the internal structure of the material is too tight, the internal flow resistance increases, leading to an increase in the reflected acoustic energy and a decrease in the transmitted acoustic energy, which results in a decrease in the sound-absorption coefficient.

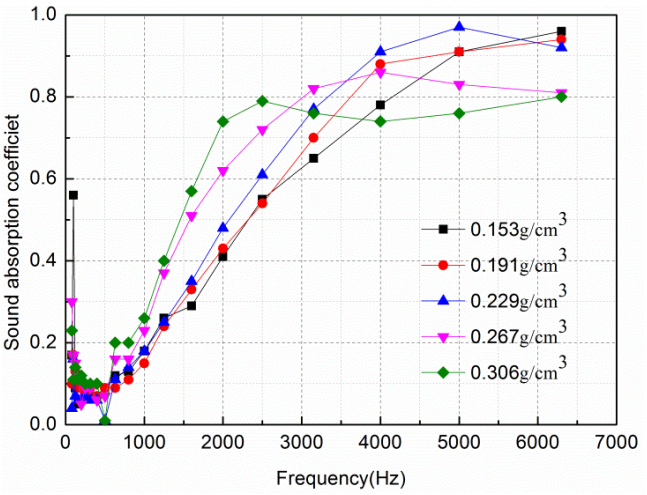

Figure 3. Sound-absorption-coefficient curves for composite materials with different densities.

3.1.2 Effect of the Mass Fraction of Waste-Wool Fibers on the Sound-Absorption Coefficient

Under technological conditions consisting of a volume density of 0.229 g·cm^{-3} and a material thickness of 10 mm, composite materials with mass fractions of waste-wool fibers of 0%, 30%, 40%, 50%, 60%, 70%, and 100% were prepared. Figure 4 shows the calculated porosity of composite materials with different mass fractions of waste-wool fibers. An increase in the mass fraction has a certain influence on the porosity of the composite materials. When the mass fraction of waste-wool fibers increased from 0% to 100%, the porosity increased from 80.59% to 83.45%. This is because the voids in a unit volume of materials containing pure waste-wool fibers (mass fraction = 100%) are larger than those in the materials containing pure waste low-melting-point polyamide fibers, so the porosity of the composite materials increases with an increase in the mass fraction of waste-wool fibers.

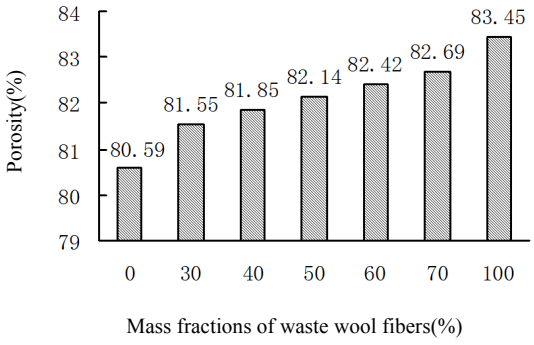

Figure 4. Porosity of composite materials with different mass fractions.

Figure 5 shows the sound-absorption-coefficient curves of composite materials with different mass fractions. It can be seen from Figure 5 that the sound-absorption coefficient gradually moves in the low-frequency direction. This is because the surface of the waste-wool fibers is relatively rough for the scale. When a sound wave passes through the waste-wool fiber, it increases both the friction and the heat loss, and therefore, the sound-absorption performance is good. However, the polyamide fibers have a smooth surface and show less resistance when sound waves pass through, so their sound-absorption performance is lower. Therefore, with an increase in the mass fraction of waste-wool fibers, the sound-absorption curve of the composite materials approaches the curve of pure waste-wool fibers and gradually tends to be flat. To sum up, when the mass fraction of waste-wool fibers is 30% and 50%, the sound-absorption performance of the composite materials is better. If the mass fraction of the waste-wool fibers is too high, it is not possible to ensure sufficient contact between the fibers. Therefore, the selected mass fraction of the waste-wool fibers was 50%.

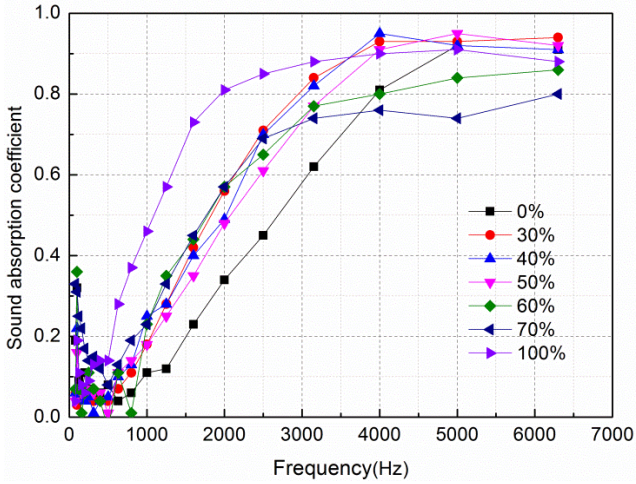

Figure 5. Sound-absorption-coefficient curves for composite materials with different mass fractions.

3.1.3 Effect of the Thickness on the Sound-Absorption Coefficient

Under technological conditions consisting of a volume density of 0.229 g·cm^{-3} and a mass fraction of waste-wool fibers of 50%, composite materials with thicknesses of 5, 10, 15, 20, 25, 30, and 35 mm were prepared. Figure 6 shows the sound-absorption-coefficient curves for composite materials with different thicknesses. It can be seen from Figure 6 that with an increase in the thickness, the peak of the sound-absorption coefficient rapidly moves in the low-frequency direction, and the effective sound-absorption frequency range is expanded [32]. However, when the thickness reached 20 mm, the sound-absorption-coefficient curve in the middle-frequency and high-frequency bands basically tended to be stable. At frequencies below 1500 Hz, the sound-absorption coefficients increased with an increase in the thickness of the composite materials, and the amount of increase was remarkable. At frequencies above 1500Hz, the sound-absorption-coefficient curves gradually tended to be stable with an increase in the thickness.

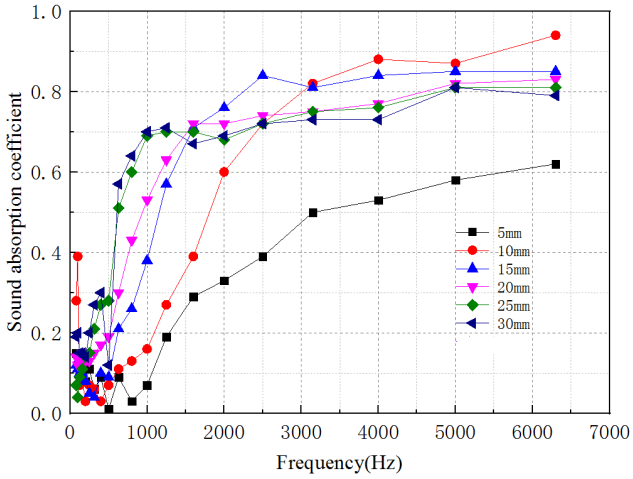

Figure 6. Sound-absorption-coefficient curves for composite materials with different thicknesses.

The reason for this observation is that low-frequency sound waves have a longer wavelength, the distance between the sound wave and the material increased, and the blockage caused by pore bending increased. Therefore, low-frequency sound waves are mainly absorbed by the interior of the composite material. High-frequency sound waves have a short wavelength and are mainly absorbed by the surface of the composite materials [33]. Therefore, an increase in the material thickness can effectively improve the low-frequency sound-absorption performance but has less influence on the high-frequency sound-absorption performance. To sum up, considering the cost of the raw materials and other factors, the thickness of the composite materials was set to 15 mm.

3.2 Fractal Characterization Results

Figure 7. Schematic diagram showing the fractal distortion of α-keratin inside waste-wool fibers

The waste-wool fibers were distorted macroscopically, and this change had self-similarity. Its inherent natural distortion was a unique fractal structure, which was fractal dimension change in accordance with fractal theory [34].

Figure 7 shows a schematic diagram of the fractal distortion of α-keratin inside waste-wool fibers. There are four layers between the wool's cortical cells and the basic fibrils, and the difference of each layer was about 10 times. The first distortion was α-keratin with a diameter of 1 nm, which was not an integer dimension. Each fibril consisted of three mutually twisted α-keratin units, and the low-density matrix (about 36%) was filled in between keratins, basic fibrils, fibrils, and microfibers. Three α-keratins in the basic fibrils occupied the remaining space (about 64%), which might be due to stress transmission caused by the natural twisting of α-keratins. About 10 basic fibrils in the microfibers were arranged in parallel, accounting for about 64% of the cross-sectional area. Similarly, the cross-sectional area occupied by microfibers and large fibrils was about 64% of that of large fibrils and cortical cells, so that a wool self-similar fractal dimension could be calculated [35]. The fractal structures of waste-wool fibers and synthetic fibers are essentially different. Synthetic fibers (including waste low-melting-point polyamide fibers) show one-dimensional, two-dimensional, or even three-dimensional integer dimensional changes. The inherent natural distortion of waste-wool fibers had non-strict self-similarity. In statistical sense, its whole and shape had self-similarity. Although it also had complex details in nanometer scale, it was difficult to describe such details with traditional geometry, that was, irregularities [36]. Therefore, from the microscopic to the macroscopic physical structure, the composite materials prepared using waste-wool fibers and waste low-melting-point polyamide fibers exhibited obvious fractal characteristics, and the sound-absorption performance of the composite materials could be forecasted by the fractal method.

3.2.1 Image Acquisition of the Composite Materials

The composite materials were thick and exhibited a large unit area. Natural light could not penetrate, so it was difficult to explore the internal structure. Therefore, a JEOL JSM-6460LV scanning electron microscope was used to obtain images of the composite materials at a magnification of 50 times. After image processing, the basal plane fiber layer was taken for pore-structure analysis. This treatment was based on the fact that the composite materials consisted of many layers of fibers with arbitrary orientation. It was assumed that most of the fiber layer aggregates were perpendicular to the propagation direction of the sound waves. Some properties (such as the sound-absorption properties) of the single layer (base plane fiber layer) could reflect the properties of the entire composite materials.

Figure 8 shows scanning electron microscopy (SEM) images of composite materials with volume densities of 0.153, 0.191, 0.229, 0.267, and 0.306 $g \cdot cm^{-3}$ (a–e).

Figure 9 shows SEM images of composite materials with different mass fractions of 0%, 30%, 40%, 50%, 60%, 70%, and 100% (a–g).

Figure 10 shows scanning electron microscopy images of composite materials with different thicknesses of 5, 10, 15, 20, and 25 mm (a–e).

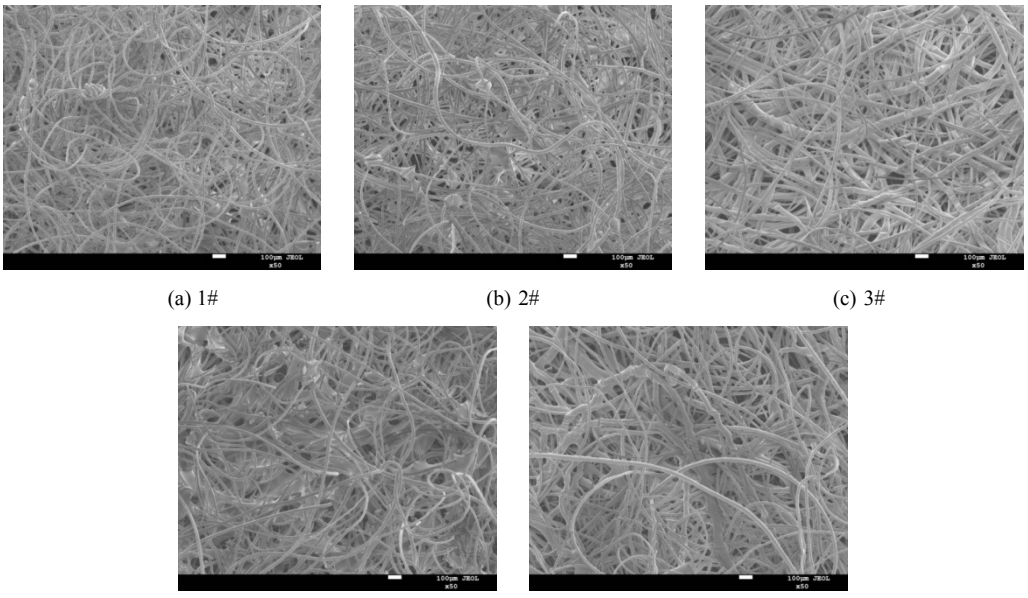

(a) 1# (b) 2# (c) 3#

(d) 4# (e) 5#

Figure 8. Scanning electron microscopy images of composite materials with different volume densities.

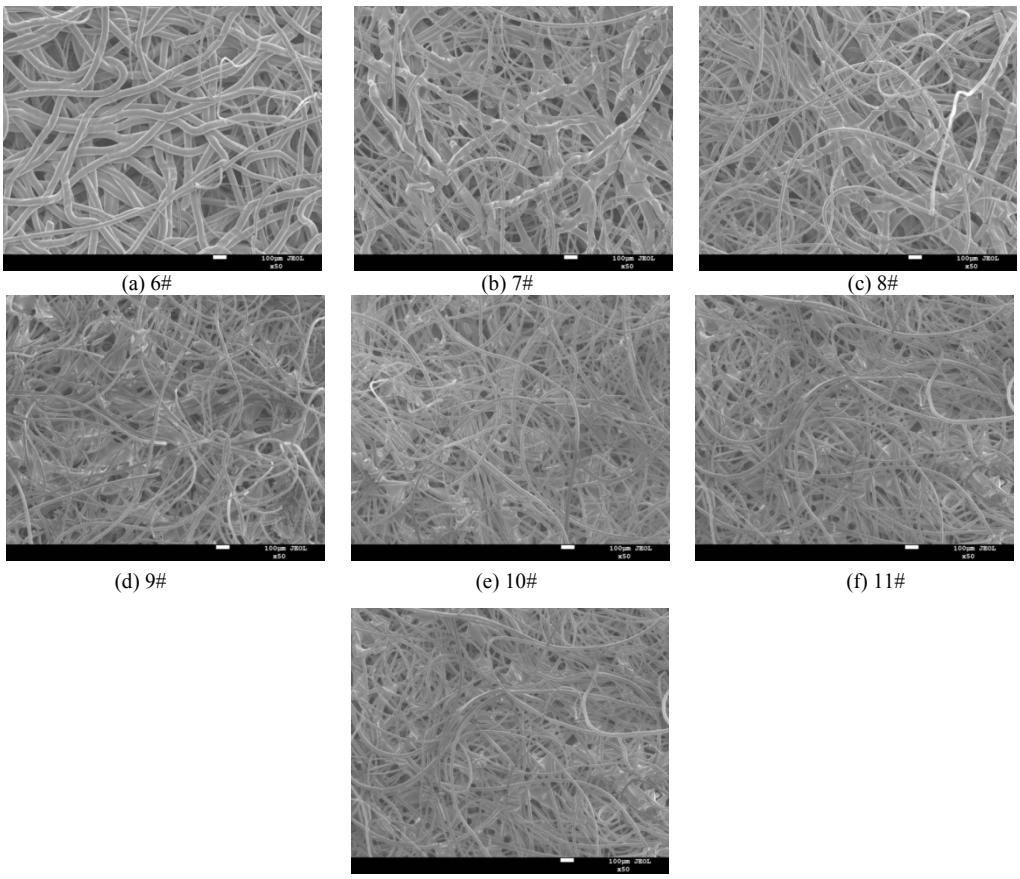

(a) 6# (b) 7# (c) 8#

(d) 9# (e) 10# (f) 11#

(g) 12#

Figure 9. Scanning electron microscopy images of composite materials with different mass fractions.

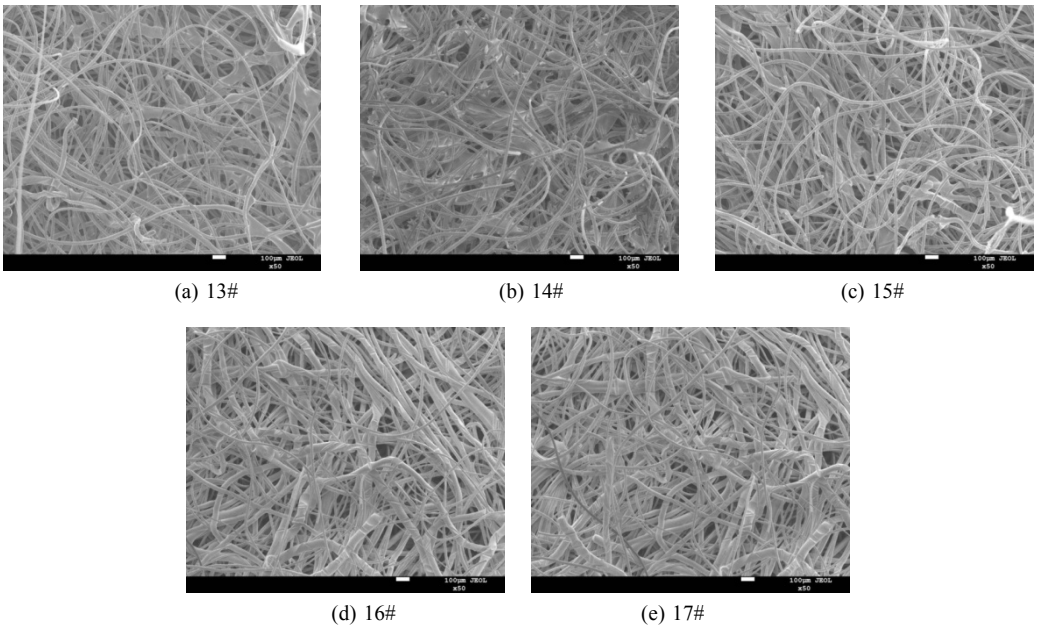

(a) 13# (b) 14# (c) 15#

(d) 16# (e) 17#

Figure 10. Scanning electron microscopy images of composite materials with different thicknesses.

3.2.2 Pretreatment of the Images of the Composite Materials

Pretreatment of the images of the composite materials was mainly performed to enhance the contrast between fibers and pores. Firstly, the SEM images of the composite materials taken under various conditions were converted into gray-scale images, and the images were enhanced by expanding the gray-scale range to the whole gray-scale area, so that the contrast of pixels in the range was obvious, the bright areas were brighter, and the dark areas were darker. Next, the histogram distribution of the images was equalized by histogram equalization to increase the gray-

value range of the composite-material images to further enhance the overall contrast of the images. Finally, median filtering was carried out on the previously processed images to eliminate isolated noise and reduce image blur [37].

3.2.2.1 Eliminating the Background

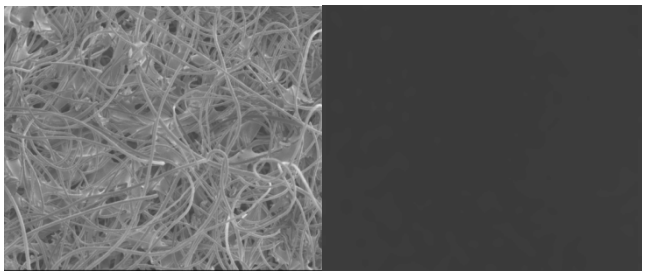

(a) **(b)**

Figure 11. Eliminating the background.

An uneven surface or an uneven illumination distribution of the composite materials can easily cause brightness differences throughout the whole image, which has a great influence on the further processing and analysis of the image. Therefore, it was necessary to eliminate the background before enhancing the image. In other words, when collecting images of the composite materials, images of the composite-materials sample were taken under the same shooting conditions. Figure 11(a) shows an original image, and Figure 11(b) shows an image of the background without sample. The effect of an uneven background can be eliminated by subtracting the two images.

3.2.2.2 Enhancement of the Images

Figure 12 shows an original image and its gray-scale histogram. As can be seen in Figure 12, the contrast ratio of the SEM image is too low, which confuses fibers and pores, but the gray-scale stretching technology can be adopted to maximize the contrast ratio of the image

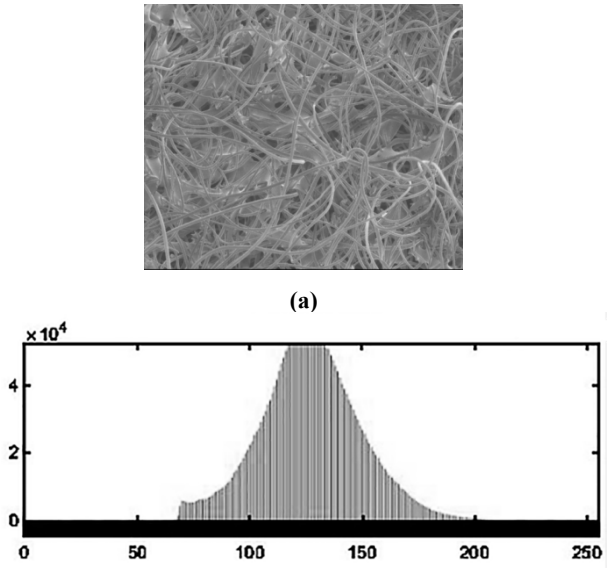

(a)

(b)

Figure 12. Original image and its gray-scale histogram.

After gray-scale stretching, the gray-scale histogram with the original concentrated distribution was stretched between 0 and 255, the distribution became more uniform, and the contrast of the image was significantly improved. Figure 13 shows the image after gray-scale stretching and its gray-scale histogram. As can be seen in Figure 13, the differences between the fibers and the pores became very clear, which was conducive to the binarization of the image in the next step

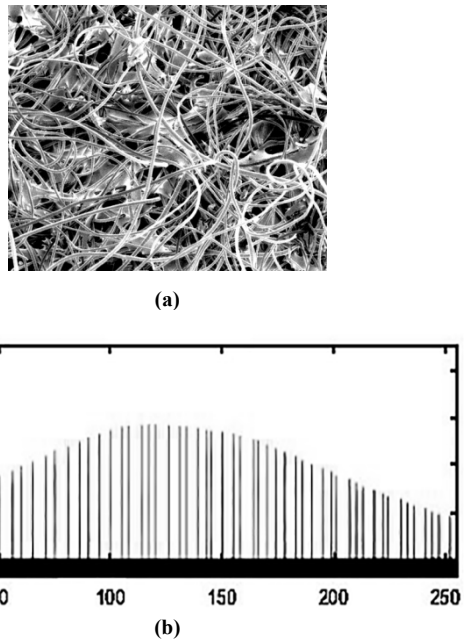

(a)

(b)

Figure 13. SEM image after gray-scale stretching and its gray-scale histogram.

3.2.2.3 Binarization of the Images

The images were divided into 256 gray levels, black was represented by 0, white was represented by 255, and the other colors were represented between 0 and 255. Image binarization refers to the setting of a threshold value. At the same time, the threshold value is used as a threshold to convert the image (multi-gray level) into a black-and-white image (two-gray level). The color of each pixel was set to black or white, and the pixel values were 0 and 1, respectively. Differences in the threshold setting methods would lead to differences in the binarization process, so the threshold should be selected reasonably. The way to divide the pores and fibers was to binarize the composite-material images by converting the points with gray value greater than or equal to the threshold value into white points (gray level 255) and the points with gray value less than the threshold value into black points (gray level 0). This topic was based on the threshold set artificially by the gray distribution map, that is, the designated threshold was 0.43, as shown in Figure 14(a). Of course, the maximum variance between classes method could also be used to calculate the threshold value of gray images, as shown in Figure 14 (b). This method was set to 255 when the gray value of a certain point was greater than the threshold value, and set to 0

when it was less than or equal to the threshold value. This was mainly done to automatically set and easily weaken the contrast of images under the same factor. Therefore, this paper adopted the method of specifying the threshold value [38].

3.2.3 Calculation of the Fractal Dimension

Figure 15 shows the calculation process for obtaining the fractal dimension.

3.2.4 Relationship between Fractal Dimension and Various Factors

3.2.4.1 Relationship between Fractal Dimension and Volume Density

Table 1 shows relevant parameters of the samples obtained with different volume densities. Figure 19 shows the relationship between the fractal dimension of the samples and the maximum sound-absorption coefficient for different volume densities.

As can be seen in Figure16, with an increase in the volume density, the fractal dimension and the maximum sound-absorption coefficient of the samples all showed a decreasing trend. The fractal dimension of the sample pores was linearly related to the average pore size (i.e. porosity). If the volume density of the sample was larger, the porosity was smaller, the pore structure was denser, and the pore fractal dimension was smaller. When exploring the influence of the volume density on the sound-absorption performance of the composite materials, the peak of the sound-absorption coefficient moved to the low-frequency direction with an increase of the volume density. When the volume density of the sample was $0.229 \cdot cm^{-3}$, the combination of the hole shape and the aperture size of the composite materials improved the sound-absorption performance throughout the whole sound-absorption frequency band. The peak of the maximum sound-absorption coefficient appeared in the test frequency range, which made the maximum sound-absorption coefficient higher but did not affect the overall trend.

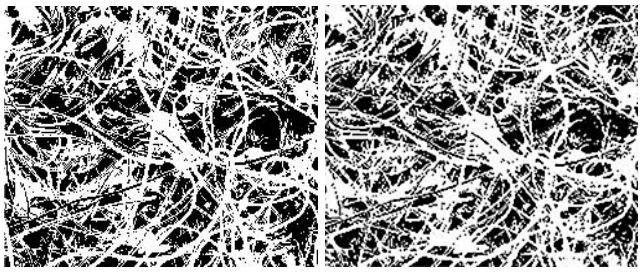

(a) (b)

Figure 14. Images after binarization.

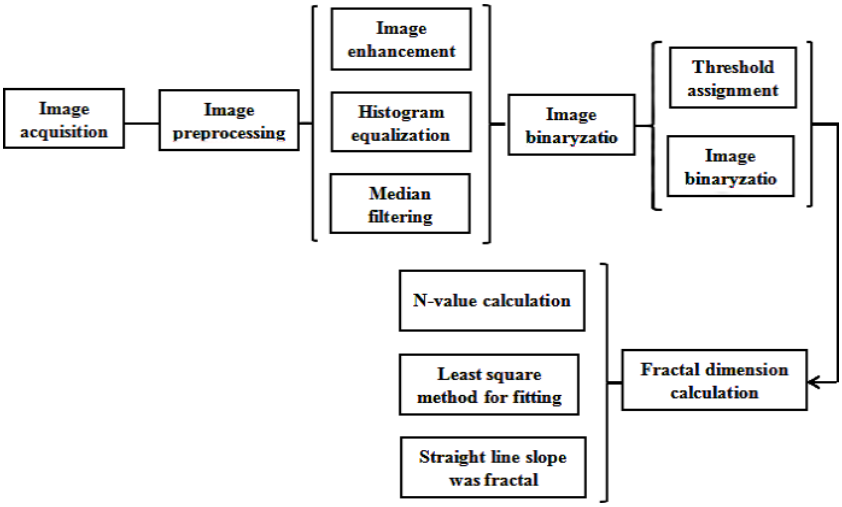

Figure 15. Calculation process for obtaining the fractal dimension.

Table 1. Relevant parameters of samples with different volume densities

Sample number	Volume density [g·cm^{-3}]	Maximum sound-absorption-coefficient	Porosity[%]	Fractal dimension	R^2
1#	0.153	0.96	88.06	1.913	0.9983
2#	0.191	0.94	85.10	1.901	0.9980
3#	0.229	0.95	82.14	1.923	0.9987
4#	0.267	0.86	79.17	1.889	0.9971
5#	0.306	0.80	76.13	1.875	0.9972

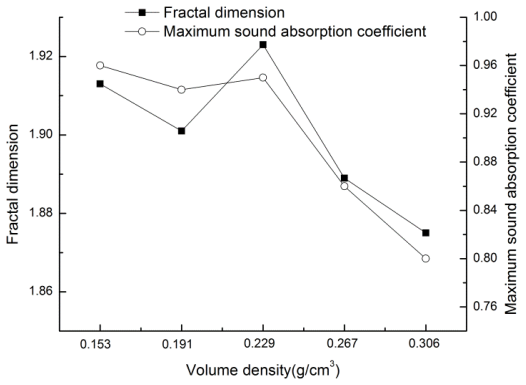

Figure 16. Relationship between fractal dimension and maximum sound-absorption coefficient for samples with different volume densities.

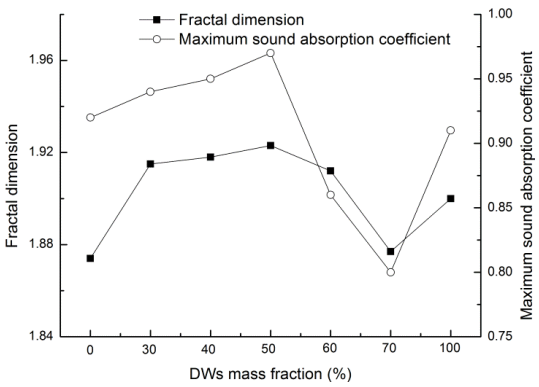

Figure 17. Relationship between fractal dimension and maximum sound-absorption coefficient for samples with different mass fractions of waste-wool fibers.

3.2.4.2 Relationship between the Fractal Dimension and the Mass Fraction of Waste-Wool Fibers

Table 2 shows relevant parameters for samples with different mass fractions of waste-wool fibers. Figure 17 shows the relationship between the fractal dimension and the maximum sound-absorption coefficient of samples with different mass fractions of waste-wool fibers. It can be seen from Figure 17 that samples 6# and 12# were samples with mass fractions of waste-wool fibers of 0% and 100%, respectively, being different from the other samples. They did not participate in the relationship between the maximum sound-absorption coefficient and the fractal dimension and were only analyzed as comparison samples. The fractal dimension was consistent with the variation trend of the maximum sound-absorption coefficient and had a linear correlation. The maximum sound-absorption coefficient was obtained at the best mass fraction of waste-wool fibers. When the mass fraction of waste-wool fibers was 0%, the fractal dimension was low, which is due to the fact that when pure polyamide fibers are prepared, the fibers melt and shrink when heated, the pore diameter of the material decreases, and the pore fractal dimension is small. Similarly, it can be explained that with an increase in the mass fraction of waste-wool fibers, the influence of the composite materials decreases, the internal complexity of the material decreases, and the pore fractal dimension slightly increases. If the mass fraction of waste-wool fibers is above 50%, the composite materials are less affected by heat, the number of pores between fibers increases, and the fractal dimension decreases accordingly.

3.2.4.3 Relationship between Fractal Dimension and Thickness of the Composite Materials

Table 3 shows relevant parameters for samples with different thicknesses. Since the thickness of the composite materials has a great influence on their sound-absorption performance, the sound-absorption-coefficient curve shifted in the low-frequency direction with an increase in the thickness. The maximum sound-absorption coefficient of the composite materials did not change significantly with the thickness, so the relationship between the fractal dimension and the resonant sound-absorption frequency corresponding to the turning point of the sound-absorption coefficient was explored.

Figure 18 shows the relationship between the fractal dimension and the resonant sound-absorption frequency for samples with different thicknesses. From Figure 18, it can be concluded that the fractal dimension has a good correlation with the sound-absorption resonance frequency, indicating that the turning point of the sound-absorption performance of the composite materials can be explored through the fractal dimension. As the thickness of the composite materials increased, the corresponding fractal dimension decreased, and the resonance frequency corresponding to the turning point moved to lower frequencies. The reason for this might be that the thickness of the composite materials was increased, the length of the channel of the acoustic wave entering the inside of the material was prolonged, and the depth of the hole was increased, thereby reducing the fractal dimension.

Table 2. Relevant parameters of samples with different mass fractions of waste-wool fibers.

Sample number	Mass fraction of waste-wool fibers [%]	Maximum sound-absorption-coefficient	Porosity[%]	Fractal dimension	R^2
6#	0	0.92	80.59	1.874	0.9972
7#	30	0.94	81.55	1.915	0.9987
8#	40	0.95	81.85	1.918	0.9986
9#	50	0.95	82.14	1.923	0.9987
10#	60	0.86	82.42	1.912	0.9981
11#	70	0.80	82.69	1.877	0.9967
12#	100	0.91	83.45	1.900	0.9978

Table 3. Relevant parameters for samples with different thicknesses of the composite materials.

Sample number	Thickness of composite material [mm]	Resonance sound-absorption frequency	Fractal dimension	R^2
13#	5	6300	1.949	0.9994
14#	10	4000	1.923	0.9987
15#	15	2000	1.915	0.9987
16#	20	1500	1.914	0.9985
17#	25	1250	1.907	0.9982

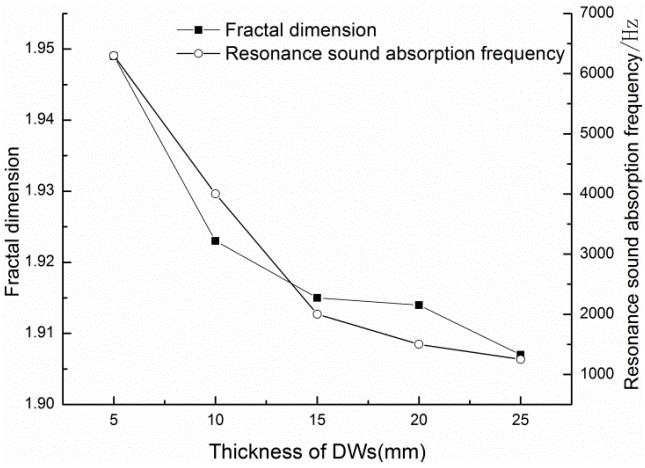

Figure 18. Relationship between the fractal dimension and resonant frequency for samples with different thicknesses.

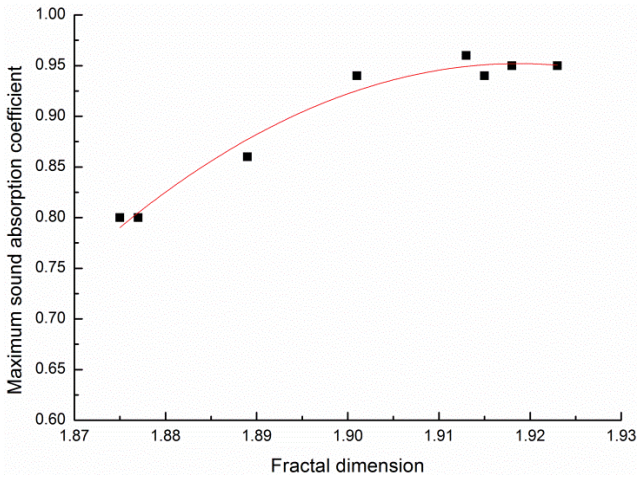

Figure 19. Fitting curve between fractal dimension and maximum sound-absorption coefficient

3.2.5 Relationship between Fractal Dimension and Maximum Absorption Coefficient

Due to the influence of deviations when acquiring images, the images with larger deviations were selected, and a relationship curve between the fractal dimensions of samples 1#, 2#, 3#, 4#, 5#, 7#, 8#, and 11# and the maximum sound-absorption coefficient was established. The fractal dimension was fitted to the maximum sound-absorption coefficient, and the fitting curve is shown in Figure 19.

The fitting relation was as follows:

$$Y = -84.375X^2 + 323.796X - 309.695 \quad (3)$$

where Y is the maximum sound-absorption coefficient and X is the fractal dimension.

The correlation coefficient between the fractal dimension and the maximum sound-absorption coefficient was 0.9741, which shows that there is a strong positive correlation between the fractal dimension and the maximum sound-absorption coefficient. In the actual design of composite materials, the fitting relation obtained above could be used to predict the maximum sound-absorption coefficient of the composite material.

A relationship curve between the fractal dimensions and the resonance absorption frequencies of samples 13#, 14#, 15#, 16#, and 17# was established. The fractal dimension was fitted to the resonance sound-absorption frequency, and the fitting curve is shown in Figure 20.

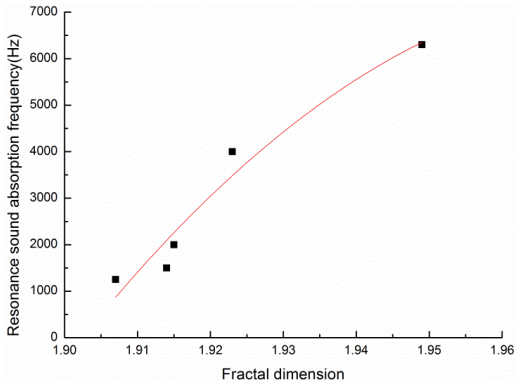

Figure 20. Fitting curve between fractal dimension and resonance sound-absorption frequency.

The fitting relation was as follows:

$$Y = -1266600X^2 + 5014500X - 4955600 \quad (4)$$

where Y is the resonance sound-absorption frequency and X is the fractal dimension.

The correlation coefficient between the fractal dimension and the maximum resonance sound-absorption frequency was 0.9086, which shows that there is a strong positive correlation between the fractal dimension and the resonance sound-absorption frequency. In the design of the actual thickness of a composite material, the fitting relation

obtained above could be used to predict its resonance sound-absorption frequency, that is, the turning point of the sound-absorption coefficient.

4. CONCLUSION

In this paper, the sound-absorption properties of the composite materials were studied by the transfer-function method. The results of single-factor experiments showed that the optimized technological conditions were: a volume density of the composite materials of 0.229 $g \cdot cm^{-3}$, a mass fraction of waste-wool fibers of 50%, and a thickness of the composite materials of 15 mm. Under the optimized technological conditions, the sound-absorption coefficients of the composite materials were above 0.8 and the sound-absorption bands of the composite materials were wide,which could be applied in the construction field, decoration field , automobile industry and so on.

The microscopic physical structure and macroscopic physical structure of the composite were analyzed, and the fractal dimensions of the composite under different factors were calculated by using the box-counting dimension method (fractal theory), the correlation coefficients were high, which showed that the structure of the composite materials containing waste-wool/polyamide fibers had strong fractal characteristics. Fractal theory was used to quantitatively characterize the complex structure of composite materials, and the relationship between fractal dimension and material density, mass fraction of waste wool fibers and material thickness were mainly analyzed. A theoretical model of structural identification index (i.e. Fractal dimension) and sound-absorption properties parameters of composite materials was established. The linear relationship between the fractal dimension and its maximum sound absorption coefficient was established as follows: $Y = -84.375X^2 + 323.796X - 309.695$, the correlation coefficient was 0.9741. The linear relationship between the fractal dimension and the resonant frequency was: $Y = -1266600X^2 + 5014500X - 4955600$, the correlation coefficient was 0.9086.Through experimental characterization and theoretical prediction analysis, the sound absorption mechanism of composite materials containing waste-wool/polyamide fibers sound absorption composites was shown. The research results provided experimental and theoretical basis for the design of sound-absorption composite materials with wide sound-absorption frequency bandwidth and high sound-absorption coefficient.

Funding: This research is funded by the Science and Technology Innovation Fund Project of Dalian (2019J12SN71).

Conflicts of Interest: The authors declare no conflict of interest.

REFERENCES

1. Tian CY, Wang F, Rong VH. 2005. Discussion on Sustainable Development Countermeasures of Fine Wool Sheep Industry in Inner Mongolia. *Animal Husbandry and Feed Science*, 26(4), 48.
2. Zhangye Comprehensive Test Station of National Wool Sheep Industry Technology System. 2017. Development Trend and Policy Suggestions of National Wool Sheep Industry in 2017. *Gansu Animal and Veterinary Sciences*, 47(4), 27-28.
3. .Jiang ZH. 2002. Japan Developed a Technology to Use Scrap Wool & Feather *China Resources Comprehensive Utilization*, (2), 8.
4. Alzeer M, MacKenzie KJ. 2012. Synthesis and mechanical properties of new fibre-reinforced composites of inorganic polymers with natural wool fibres. *Journal of Materials Science*, 47(19), 6958-6965.
5. Patnaik A, Mvubu M, Muniyasamy S, Botha A, Anandjiwala RD. 2015. Thermal and sound insulation materials from waste wool and recycled polyester fibers and their biodegradation studies. *Energy and Buildings*, 92, 161-169.
6. Li Y, Zhang DK. 2018. Preparation of wet-laid nonwoven fabric using super-short waste wool fiber. *Journal of Xi'an Polytechnic University*, 32(6), 623-627.
7. He YZ, Wang HF. 2012. Research for recycle process of waste wool fiber. *Wool Textile Journal*, 40(9), 14-17.
8. Yao JB, He TH. 2003. Preparation of wool's keratin solution. *Wool Textile Journal*, (4), 16-19.
9. Jia JR, Yao JB. 2015. The latest progress in research of recycling scrap of wool keratin. *Wool Textile Journal*, 43(1), 45-49.
10. Sun YL, Yao JB, Li B, Jia SG. 2015. Application of wool keratin solution in wool fabric shaping. *Journal of Textile Research*, 36(4), 97-101.
11. Li K, Wang M. 2018. Preparation and properties of blended membrane based on abandoned wool protein. *Dyeing and Finishing,* 44(5), 8-23.
12. Lv LH, Liu YJ, Li CT, Guo J, Ye F. 2019. Properties of Waste Fiber/Polyurethane Flame Retardant Insulation Board. *Tekstil ve Konfeksiyon,* 29(2), 152-161.
13. Lv LH, Bi JH, Ye F, Qian YF, Zhao YP, Chen R, Su XG. 2017. EXTRACTION OF DISCARDED CORN HUSK FIBERS AND ITS FLAME RETARDED COMPOSITES. *Tekstil ve Konfeksiyon*, 27(4), 408-413.
14. Cheng G. 2009. Performance and application of wool sound absorption and thermal insulation product. *New Building Materials*, 36(5), 63-66.
15. Luan QL, Qiu H, Cheng G, Ge MQ. 2016. Preparation and sound absorption properties of waste wool nonwoven material. *Journal of Textile Research*, 37(7), 77-81.
16. Luan QL, Qiu H, Cheng G, Ge MQ. 2016. Preparation of porous sound absorbing material based on discarded wool fiber. *Chinese Journal of Environmental Engineering*, 10(10), 6081-6086.
17. Luan QL, Qiu H, Cheng G, Liu XY. 2017. Sound absorption properties of nonwoven material based on wool and its hybrid fibers. *Journal of Textile Research*, 38(3):67-71.
18. Burrough PA. 1981. Fractal dimensions of landscapes and other environmental data. *Nature*, 294(5838), 240-242.
19. Milne BT. 1988. Measuring the fractal geometry of landscapes. *Applied Mathematics and Computation*, 27(1), 67-79.
20. West BJ, Goldberger AL. 1987. Physiology in fractal dimensions. *American Scientist*, 75(4), 354-365.

21. Du CJ, Sun DW. 2004. Recent developments in the applications of image processing techniques for food quality evaluation. *Trends in food science & technology*, 15(5), 230-249.

22. Yang XH. 2003. Expression and Fractal Simulation of Morphologic Structures of Nonwovens (Doctoral dissertation). Available from CNKI and Wangfang database. (DOI:10.7666/d.y645366).

23. Wang YH. 2018. T700/BMI Porosity Detection and Fractal Research of Pore Morphology Feature (Master's thesis). Available from CNKI and Wangfang database. (DOI:10.7666/d.y01662570).

24. Lyu L, Liu Y, Bi J, Guo J. 2019. Sound Absorption Properties of DFs/EVA Composites. *Polymers*, 11(5), 811.

25. Yang S, Li MS. 2017. Relationship between fractal structure and warmth retention properties of wool fiber assembly. *Journal of Textile Research*, 38(08), 11-15.

26. Chen L, Jiang Z, Jiang S, Liu K, Yang W, Tan J, Gao F. 2019. Nanopore Structure and Fractal Characteristics of Lacustrine Shale: Implications for Shale Gas Storage and Production Potential. *Nanomaterials*, 9(3), 390.

27. Lyu LH, Li CW, Wu CX. 2018. Preparation of Discarded Peanut Shell/EVA Composite and Its Sound Absorption Properties. *Advanced Textile Technology*, 26(4), 12-16.

28. Ma YX. 2010. STUDY ON SOUND ABSORPTION PROPERTIES OF COMPOSITE NEEDLE-PUNCHED NONWOVENS (Master's thesis). Available from CNKI and Wangfang database. (DOI:10.7666/d.y1864290).

29. Sun X, Wu ZQ, Huang Y. 2003. Fractal and cone. In 2 Editor (Ed.), *Fractal Principle and Its Application*. Anhui, China: China University of Science and Technology Press, 23–41.

30. Li HT, Deng Y. 2002. Fundamentals of M-File Programming. In 8 Editor (Ed.), *Matlab program Tutorial*. Beijing, China: Higher Education Press, 187-213.

31. Li CW, Lyu LH. 2018. Preparation and properties of sound absorption composites based on waste wool. *Journal of Textile Research*, 39(10), 74-80.

32. Zhao M. 2004. Mechanical Noise Control Technology. In 9.2 Editor (Ed.), *Mechanical Vibration and Noise.* Beijing, China: Science Press, 221–223.

33. Peng LM, Wang JF, Fu F, Wang D, Zhu GY. 2015. Experimental Study on Sound Absorption of Wood Fiber/Polyester Fiber Composite Materials. *Journal of Building Materials*, 18(1), 172-176

34. Mandelbrot BB. 1983. The fractal geometry of nature/Revised and enlarged edition. New York, *WH Freeman and Co*., 1983, 495.

35. Gao XS, Tong Y, Zhuang Y, Hong JQ. 2000. THE FRACTAL STRUCTURE OF NATURAL FIBERS AND THE DEVELOPMENT OF FIBER WITH FRACTAL STRUCTURE. *CHINA SYNTHETIC FIBER INDUSTRY*, 23(4), 35-38.

36. Zhang JZ. 2011. *Fractal*. Beijing, China: Tsinghua University Press.

37. Yang S, Yu WD, Pan N. 2010. Effect of nonwovens pore fractal dimensions on their acoustic absorption behaviors. *Journal of Textile Research*, 31(12), 28-32, 38.

38. .Gao G, Zhong HJ, Song XJ, Liu XR, Mi XQ. 2005. Fractal characteristic analysis of non-woven fabrics. *Journal of Tianjin Polytechnic University*. 24(2):86-88.